Carbonation of filler typed self-compacting concrete and its impact on the microstructure by utilization of 100% CO_2 accelerating techniques

Mahmoud Khashaa Mohammed*, Andrew Robert Dawson, Nicholas Howard Thom

School of Civil Engineering, Faculty of Engineering, University of Nottingham, University Park, Nottingham NG7 2RD UK, E-mail: evxmkm@nottingham.ac.uk, Lecturer, University of Anbar, Iraq, Faculty of Engineering, E-mail: mahmoudkh_ani@yahoo.com

*corresponding author

Abstract

Via the use of accelerated carbonation techniques with 100% CO_2 concentration, an experimental programme was performed to investigate the carbonation and associated microstructural changes of three different Self-Compacting Concrete (SCC) in which some of the cement had been replaced by limestone powder, fly ash and/or silica fume . Accelerated carbonation tests were conducted on these “filler-typed” SCCs after 28 days water curing .Approximately 33% of the total binder (450 kg/m^3) was replaced by limestone powder, fly ash or a fly ash-silica fume blend.

The results revealed that the replacement of limestone powder (LP) increased the depth of carbonation during the accelerated test relative to the effect of the fly ash (FA) or the combination of the fly ash and the silica fume (FA+SF) replacements. However, the modelling of the normal pressure accelerated carbonation tests with 100% CO_2 showed all the SCCs studied have no risk of carbonation induced corrosion in the natural environment. Overall, the research suggests that carbonation of filler typed SCC may not be chemically controlled, rather, the internal pore structure may play an important role. Furthermore, the effect of carbonation on the internal pore structure and the chemistry of the concrete matrices were more noticeable in SCC containing FA+SF than in those with LP and FA replacements.

Keywords: accelerated carbonation, 100% CO_2, self-compacting concrete; microstructure; pore size distribution; cement replacement

1. Introduction

The durability of self-compacting concrete SCC structures exposed to aggressive environmental conditions is still a major concern of many concrete investigators [1-3]. Carbonation, beside chloride attack has been considered as one of the most disruptive phenomena that can affect the concrete durability, potentially causing a significant reduction in service life [4, 5]. Until now, the carbonation of SCC is a somewhat controversial topic. SCC has sometimes a larger and sometimes a smaller carbonation penetration as compared with the Normal Vibrated Concrete (NVC) at the same strength level. Based on previous experimental works, the high amount of CH and CSH found in SCC might reduce the carbonation hazard[6]. However, this might mainly depend on the type of filler and its impact on the composition of the cement paste. Substantial research work [7, 8] has reported that a beneficial outcome of carbonation is in reducing the porosity and improving the microstructure of the cementitious materials.

The macro and micro diffusivity properties of the concrete may alter due to the change of the porosity and the pore distribution caused by the carbonation process. Furthermore, carbonation might cause a significant alteration in the concrete properties that are strictly related to the microstructure, such as the capillarity of the pores in addition to the change of the pH of the pore solution. The change in the pore solution has a strong effect on the concentration of the destructive ions such as sulphate and chlorine. However, in aggressive environments, the permeability and diffusivity of the concrete is mainly governed by the capillary pores and their interconnectivity[9, 10]. Another form of carbonation attack comprises the neutralization of the alkalinity (pH value) of the hydrated cement paste. The process consists of the diffusion of the gas through the pores system and then the reaction with the hydration products especially CH in the presence of water. Carbonation can cause the pH value of pore water inside the concrete to decrease to about 8.3. This will terminate the passive layer of the embedded steel and permit the corrosion of steel rebar to commence [11, 12].

According to Stehlik et. al [13] and Matouek and Drochytka (1998), there are four stages in the carbonation process of concrete. The first stage is the reaction between carbon dioxide and the calcium hydroxide in the presence of humidity as shown in Equation 1:

$$Ca(OH)_2 + CO_2 + H_2O \bullet\!\!\longrightarrow CaCO_3 + 2\ H_2O \ldots\ldots\ldots\ldots (1)$$

The second stage (Equation 2) is the transformation of the insoluble resulting $CaCO_3$ into a soluble phase:

$$CaCO_3 + CO_2 + H_2O \longrightarrow Ca(HCO3)_2 \ldots\ldots\ldots\ldots \quad (2)$$

The third stage consists of recrystallizing the resulted insoluble carbonates to large calcite and aragonite crystals and the fourth stage is referred to as full carbonation (100% carbonation). It is important to highlight that the first stage has a significant impact on the porosity and permeation properties of the concrete because of the crystallization of $CaCO_3$ in the pores. Yet the overall process may significantly disturb the pH level and might even alter tortuosity, porosity and pores size distribution of the matrix. The metastable calcium carbonate $Ca(HCO3)_2$ is considered as one of the main causes of the changes in the pore size distribution [9]. However, Borges et. al [14]claimed that not only may the CH be attacked by CO_2, but even more the CSH gel, with the overall porosity and permeability potentially being increased if the main phase (CSH) is also attacked. The pore structure and diffusion properties of hydrated cement pastes after complete carbonation were studied by Ngala et. al. [15]. They found that there was a decline in the total porosity of three cement paste systems (Ordinary Portland cement (OPC), fly ash and slag pastes) after carbonation, but the most interesting find of their research was the redistribution of the pore sizes; the percentage of large capillary pores (diameter >30 nm) was increased somewhat for the OPC pastes while it was increased considerably more for the fly ash and slag pastes.

2. Research significance

The carbonation of the concrete is considered one of the major concrete durability problems especially with the continuous increase of CO_2 concentration in the atmosphere. Traditionally, carbonation is of concern due to its ability to reduce the service life via the initiation of the corrosion of embedded steel due to the neutralization of the pH value of the cement paste, without causing any harm to the concrete itself. However, in modern types of concrete such as High Performance Concrete (HPC), Self-Compacting Concrete (SCC) and Reactive Powder Concrete (RPC), this concern may prove to be unfounded due to the use of different reactive and non-reactive filler materials in which the impact of the carbonation on the microstructure and chemistry of the concrete may have different features.

For the SCC, and from a practical point of view, there is a lack of information about actual carbonation due to the relatively young age of SCC structures. Recently, several laboratory studies have been performed to investigate the durability characteristics of SCC including the carbonation. The most common approach has been to compare the carbonation penetration rate between SCC and NVC.

In mature SCC with a high filler-replacement rate, the question that may be raised: which has the dominant effect in determining the carbonation propensity: the chemical composition, represented by the CH content of the matrix or its pore system? In addition, how does the carbonation change the pore distribution, the microstructure and the chemistry of the carbonated SCC? Thus, the main aim of the present study is to investigate the carbonation progression of filler-typed SCC and its impact on the microstructure of the matrices. This is achieved using two types of carbonation accelerating test considering 100% CO_2 concentration along with microscopic studies.

3. Accelerated carbonation techniques

It is well known that the carbonation is a very slow process in concrete, especially in HPC and it may take a very long time to occur. Therefore, the use of accelerated carbonation becomes necessary for most concrete researchers[11, 16]. Accelerated carbonation testing is crucial to accelerate the slow reaction between CO_2 and the hydration products in cement paste. Although various standards such as the BS EN standard [17] recommend use of (4 ±0.5) % by volume of carbon dioxide concentration, temperature at (20 ± 2) ºC and relative humidity at (55 ± 5) % for the evaluation of the carbonation depth, the accelerated carbonation test has been utilized by many researchers in order to investigate the carbonation process both to compare carbonation rates of different types of cementations materials and to predict the actual carbonation rate[18-23].

It is argued by the researchers that the higher concentration of CO_2 might increase the carbonation velocity. On the other hand, others demonstrated that the high concentration may lead to rapid carbonation of the concrete surface and, consequently, this could reduce the penetration of CO_2. A 98% CO_2 concentration was successfully used by Stehlik and Novak [13] when making a correlation between the carbonation in the natural environment and in an accelerated test using Fick's first law of diffusion . Sanjuan et. al [16] pointed out that the rate of carbonation under 100 % CO_2 and a relative humidity of 60 % was 40 times than in natural condition. This was when testing the carbonation of normal vibrated concrete with cement contents of 250 kg/m^3 and 350 kg/m^3 with w/c ratios 0.69 and 0.49, respectively. For studying the carbonation induced corrosion and electrochemical re-alkalization technique after carbonation,   Al-Kadhimi et al [11] proposed a pressurised accelerated carbonation procedure with a pure atmosphere of CO_2 and a pressure up to 15 bars. They revealed that the microstructural characteristics of carbonated concrete at high pressure strictly agreed with those obtaining from naturally carbonated concrete. Thus, the proposed accelerated technique could be useful for examining the vulnerability of materials to carbonation. Accordingly, two types of accelerated testing were utilised in the present investigation:

- Normal pressurised accelerated carbonation test with 100% CO_2 for the purpose of carbonation depth monitoring and predicting the service life of the mature filler typed SCC.
- Pressurised accelerated carbonation test to study the change of pore structure, the microstructure and chemistry of the matrices after carbonation.

3.1Normal pressure accelerated carbonation test with 100% CO_2

A plastic box with dimensions 605x370x355mm was used to design a simple carbonation chamber. It had one inlet for providing the gas from a CO_2 tank and one outlet for releasing any pressure inside the box. A saturated NaCl solution was used to maintain a humidity of 75± 5 % [24]. However, the recorded humidity was between 50 to 80 % through the period of the accelerated test with a temperature between 19 -24 ºC. The specimens were stored over a steel mesh, to avoid contact with the saturated NaCl solution and the chamber was filled by CO_2 each two weeks (by allowing the exhaust valve to vent while CO_2 is injected from the inlet valve) and sealed very well to ensure 100% concentration of CO_2. A schematic diagram and photograph of the chamber are shown in Fig.1.

3.2 Pressurized accelerated carbonation test

The Pressure Aging Vessel (PAV) which is mainly used to simulate the long term aging of asphalt binder was modified as a pressurized accelerated carbonation test vessel (Fig.2). The original oxygen cylinder was replaced by a CO_2 tank to provide the vessel with 100% concentration of CO_2 at a pressure of 2.8 bars. Three SCC mortar samples discs 60 mm in diameter by 10±3 mm high with between 50-70 % partial saturation, cut from cylinders (60 x 120 mm), were used for each filler typed SCC mortars as shown in Fig. 2. One was used for monitoring the progress of the carbonation using the phenolphthalein indicator through the cross section of the specimen and the others were kept inside the vessel until complete carbonation. After approximately 15 days, a full carbonation was achieved when the phenolphthalein pink colour of a specimen disappeared completely indicating the drop of the pH value below 9.5 as recommended by RILEM[25].

4. Materials, mix design and production of the mixes

4.1 Materials

Ordinary Portland cement CEM I, 52.5 R was used to produce the SCC. Local river quartz sand with a maximum particle size of 5 mm was used as a fine aggregate for both SCC and mortars. The specific gravity and the water absorption of this type of sand were 2.65 and 1.5 %. Natural quartz uncrushed gravel with a nominal maximum size of 10 mm was used as coarse aggregate. The specific gravity and the water absorption of the gravel were 2.65 and 0.8 %. Natural limestone filler come from Longcliffe quarry (Derbyshire, UK) with a particle size less than 65 µm. A fly ash produced by the Cemex Company had a density of 800-1000 kg/m^3. Densified silica fume produced by the Elkem Microsilica Company was used with a bulk density 500-700 kg/m^3 and more than 90% SiO_2 content was used at a dosage of 10% of the cement in case (partially replacing the fly ash) . Polycarboxylate-based superplasticizer was used in all mixes. Several trial mixes were conducted to obtain these selected dosages of SP.

4.2 Mix design and production of SCC mixtures

Table 1 shows the mix proportions, the fresh properties tested and the 28 day compressive strength of the SCC studied. The same amount of water was used in all SCC batches. For the mortar specimens, the amount of water was reduced by 0.8 % (coarse aggregate absorption) to ensure the same water to binder ratio as for the full SCC.

Slump flow diameter and the time taken to reach a slump diameter of 50cm, T_{50}, were used to assess the flowability of the mixes. The fresh SCC and mortars were filled into the moulds without any compaction. Thereafter, the specimens were left in their moulds for 48 hours, and finally cured at 20±2 ºC in a water tank for 28 days.

5. Experimental work

5.1 TGA, MIP and SEM tests at 28 days

Powder samples (that passed through a 75μm sieve) and small mortar pieces weighing 1- 3g were taken from the middle part of healthy 70 mm mortar cubes before the accelerated carbonation test and used for the Thermo Gravimetric Analysis (TGA) and mercury intrusion porosimetry (MIP) tests respectively. Similar MIP specimens were taken after carbonation. Further, SEM images were acquired to check the capillary pore structure of the matrices using plutonium-coated fractured surfaces, before carbonation. The same technique was used to identify the microstructural change of the pores after full carbonation (See 5.3).

5.2 Carbonation depth measurement

Cylindrical concrete and mortar specimens were prepared for carbonation depth measurement. The specimens had a diameter of 60 cm and a height of 120 cm. After water curing for 28 days, the top and bottom ends of the cylinders were sealed using plastic caps to ensure the radial movement of the carbonation. They were stored inside the unpressurized chamber for 240 days. At ages of 30, 60, 90, 120 and 240 days, the specimens were removed from the chamber and the following steps were conducted to observe the progression of the carbonation depth:

- After removing the plastic caps, a 15 mm long (60 mm diameter) disks were cut from the bottom side of each cylinder using a machine saw.
- The sectioned surface was cleaned from any dust and the depth of carbonation through the circumference of the disks was detected by a phenolphthalein indicator.

- The depth of carbonation was recorded as an average value of four readings taken 90º from other on the disk. In some cases especially for the concrete samples, another two readings were added to evaluate the minimum depth of carbonation. The procedure of detecting and measuring the carbonation depth is shown in Fig 3.
- The shortened cylinders were then sealed again and loaded into the chamber for further carbonation.

5.3 Tests after carbonation in the pressurised chamber

In contrast to the partially carbonated specimens obtained in the normal pressure container (Fig.1), 100% carbonated specimens were obtained from the pressurised accelerated carbonation (Fig.2). Two types of tests were conducted on these carbonated samples:

- Small pieces weighing 1-3 g from the middle part of fully carbonated mortar samples were used for the MIP test in order to detect the change of the internal pore structure compared to that already evaluated before carbonation at 28 days.
- SEM images were acquired to check the change of the morphology of the carbonated sample and to detect the change of the chemistry inside the pores using plutonium-coated fractured surfaces compared to those before carbonation.

6. Results and discussion:

6.1 Thermo gravimetric test TGA and the carbonation progress

The detected amount of CH% due to the dehydration at 420 and 550˚C of the powder samples heating to about 950˚C before the exposure to accelerated carbonation is summarised in Table 2 .The results show that the amount of CH% was significantly lower in the SCCs containing FA and FA+SF as compared with that of LP-SCC. It is well known that the reaction of such pozzolanic materials can generate additional different form of CSH due to the reaction with the CH in the presence of water [26]. Thus, this behaviour might be as a result of the higher pozzolanic activity of the FA and SF in consuming the CH compound as compared to the unreactive LP filler.

Fig. 4 represents the change of the carbonation depth of the self-compacting concretes and mortars with time as a result of testing under normal accelerating test with 100% CO_2 conditions up to 240 days. The results indicated that both LP self-compacting concretes and mortars showed the highest carbonation depth at all ages. This was followed by FA-SCC which exhibited approximately the same 28 day compressive strength as the FA-SF-SCC. However, the latter revealed the lowest carbonation depth at all test ages. Before the exposure to the accelerated carbonation, the TGA analysis demonstrated that LP-SCC exhibited the highest amount of CH due to the dehydration relative to the other two filler typed SCCs, followed by FA-SCC and FA-SF-SCC.

Chemically, this suggests that the LP-SCC should have the highest resistance to carbonation due to the high amount of CH in the cement paste which can capture the CO_2 and prevent it from further diffusion. However, physically, the analysis of the pore structure before carbonation clearly showed that this type exhibited a more porous microstructure than the other SCC mixes see Table 4. The results appear to demonstrate that modification of the pore structure in both FA and FA-SF-SCC increase the resistance to carbonation and offset the effect of reducing the CH.

6.2 predicting of actual carbonation depth

The monitoring for eight months of the carbonation depth of the filler typed SCC was used to predict the carbonation depth in a natural environment and the results are summarized in Table 3.The accelerated coefficient of diffusion for SCC mixes was calculated as the slope of the carbonation depth- square root relationship as shown in Fig. 5 according to the first Fick's law (Equation 3) which was mainly used for carbonation modelling [27]. The experimental results showed an excellent correlation factors with the regression lines (at least 96.37 %).

$$X = Kacc.\sqrt{t} \;\ldots\ldots\ldots\; (3)$$

X: Depth of carbonation (mm)

$K_{acc.}$: Carbonation coefficient (mm/√year)

t: time (year)

The actual carbonation diffusion coefficient ($K_{act.}$) was calculated using the formula developed by Sisomphon and Franke [21] for the accelerated test under 3% CO_2 concentration but here altered for 100% CO_2 concentration. The ratio of the accelerated and the actual diffusion coefficients could be stated in terms of CO_2 concentrations at the accelerated and natural conditions considering that 0.04% is the actual CO_2 concentration in the atmosphere. Fig. 6 shows the CO_2 concentration increase in the atmosphere from 1955 to June 2013 measured at Mauna Loa observatory by U.S. Department of Commerce-National Oceanic and Atmospheric Administration [28]. According to this measurement, this is the first time that the CO_2 concentration has reached to about 400 ppm in May 2013 since 1955. K_{acc}. is 50 times than $K_{act.}$ considering 100 % CO_2 (Equation 4):

$$\frac{Kacc.}{Kact.} = \sqrt{[CO2]100\,\%/[\,CO2]0.04\%} = 50 \ldots\ldots\ldots (4)$$

The analysis, Table 3, demonstrates that the predicted carbonation depths were only 5.44 mm, 4.60mm and 3.61mm for LP-, FA- and FA-SF-SCC after 50 years of exposure to natural environment. Therefore, there is no risk of carbonation-induced corrosion during the service life. If atmospheric carbon should rise to 0.06% in 50 years' time [refer to the Intergovernmental Panel on Climate Change (IPCC) worse case estimate] then these predictions rise to 6.7, 5.66 and 4.42 for LP-, FA- and FA-SF-SCC respectively (a conservative assumption as concentration is taken as 0.06% thought those 50 years). Therefore, even increased greenhouse gas isn't likely to lead the initiation of steel corrosion over the same time scale.

6.3 Quantitative analysis of the pore structure (MIP) before and after carbonation

In general, the carbonation can promote blocking of the pore structure of the matrix for the concrete. However, the incorporating of fine reactive and non- reactive filler and higher amounts of SP, such as in the case of SCC, can modify the pore structure to a large extent and the impact of the carbonation on the internal structure of the SCC might be different. Thus, it would be interesting to identify the change in pore characterization after carbonation of each SCC. Changes in the pore connectivity and pore concentration after carbonation could have a major impact on the diffusivity of water and of aggressive agents through the concrete.

Fig. 7 (a) shows the cumulative MIP intrusion volume against the pore diameter of the LP-SCC matrix while Fig. 7 (b) shows the frequency distribution of these pores. Fig. 8 (a) and (b) display the change in the pore frequency distribution for the FA and FA-SF SCC before and after carbonation.

In general, the results of MIP after carbonation demonstrated a noticeable redistribution of the pore structure of the all filler typed SCC matrices. The calculated percentages of the total pores (micro and macro pores considering 0.1μ to be the boundary between these pore classes) before and after carbonation and the CPD are presented in Table 4.

From Table 4, the results of LP-SCC indicated that the carbonation promoted the micro pores to about 18 % from the original micro pores before carbonation. In addition, the critical pore diameter (CPD) reduced from 0.06 micron to 0.027 micron .The corresponding development of the micro pores was about 3.1 % for the FA-SCC while it showed a small decrease in the CPD from 0.038 micron to 0.027 micron as compared with the LP-SCC.

On the other hand, the percentage of the micro pores in FA-SF-SCC shifted from 71 % to 79.5%. However, the most surprising result was the slight increase of the CPD for this type after carbonation from 0.031 micron to 0.038 micron. This may be as a result of the carbonation of the CSH gel which is expected to have been present at a higher percentage in this type of SCC due to the high activity of SF in consuming the CH and producing further

CSH. Perhaps the carbonation of CSH in the cement paste of this type explains the changes observed especially at the micro pores level (See Fig.9). Recently, the work conducted by Borges et.al [14] to investigate the carbonation of CH and CSH in composite cement pastes containing high amounts of blast furnace slag (BFS) indicated that overall porosity and permeability may increase if the main phase (CSH) is attacked by CO_2. If the resistance of the cement paste is sufficiently high to prevent a constant CO_2 penetration, the probability of the reaction between CO_2 and CSH might increase. On the other hand, for blended pastes with low resistance to the CO_2 access, they pointed out that carbonation of CSH having a low Ca/Si ratio might not cause a considerable change in the capillary pores structure.

6.4 Pore structure change linked with the SEM observation after carbonation

The quantitative results obtained from the cumulative MIP test intrusion volume against the pore diameter before and after carbonation are summarized in Fig. 9. The results show noticeable changes in the cumulative pore percentages especially in the range of (0-100) μ for the FA-SF-SCC matrix as compared with the other two mixes.

The SEM observations of the matrix of the FA-SF-SCC after carbonation indicated the presence of coarse pores in several areas in comparison with the matrices of the LP- and FA-SCC. The detailed SEM examination of the pores before and after carbonation of the LP- , FA- and FA-SF-SCC matrices are shown in Figs. 10, 11 and 12. The results revealed that the Ettringite occurred in the capillary pore structure in two forms after carbonation as shown in Figs. 11 and 12. Monosulfate needles, which are not an expansive form, were found in both LP- and FA- SCC cement pastes after carbonation. However, this compound was much more prominent in the pores of the LP -SCC rather than in those of the FA-SCC.

The transformation of the monosulfate into the hexagonal Ettringite shape is associated with approximately 2.3 times increase in the volume [29]. This form of Ettringite (hexagonal shape) was found in the pores of the FA-SF-SCC (Fig.12). The presence of the first form could lead to an increase in the proportion of micro pores in the LP-SCC and FA-SCC matrices and a decrease in the CPD as well.

The occurrence of the second form of the Ettringite in the FA-SF-SCC might have caused a kind of microscopic damage to the pore structure due to the expansion pressure caused by the volume increase as this form of Ettringite developed. This might, thus, be responsible for a substantial change of the pores in the range of 0.1-100 µ (See Fig. 9) and the slight increase in the CPD as detected by the MIP test.

This delayed Ettringite formation (DEF) (i.e. Ettringite not found during initial curing) could be associated with pore changes after heat-treatment, freeze-thaw attack with and without de-icing salt, sulphate attack and in the presence of the combined action of the CO_2 and water (carbonation) in the cement paste due to the low pH value. Ettringite results from the decomposition of the monosulfate in the cement paste to produce $CaCO_3$, $Al(OH)_3$,gypsum, and water. A part of original monosulfate then combines with the liberated gypsum to form the Ettringite. However, whether the formation of the this compound during the carbonation has a practical impact or not is a subject of controversy [29].

7. Conclusion and recommendations

Based on the experimental work in the present study, the following concluding remarks can be drawn:

- Under normal pressure 100 % CO_2 accelerated testing, the carbonation depth of LP-SCC or mortars was higher than FA- and FA-SF-SCC or mortars at all ages of the test. In contrast, the FA-SF-SCC revealed the lowest carbonation depth. Before the exposure to the accelerated test, the first type showed a higher amount of CH than the latter. This result might indicate that the carbonation progression in SCC is not chemically controlled but, instead, that the pore structure could play a substantial role in determining the progression of the carbonation.

- Whatever the type of the filler, whether non-reactive (LP) or reactive (FA and SF) with 33% replacement of binder, the actual predicted carbonation diffusion coefficient did not change much after 28 days water curing. Stating the finding in another way, the change of the chemistry of the matrix due to the addition of different fillers had little impact on the actual carbonation rate. Therefore, none of the filler-typed SCC mixes is at risk of carbonation induced corrosion in natural exposure. The predicted carbonation depths were only 5.44 mm, 4.6 mm and 3.61 mm for LP-, FA- and FA-SF-SCC respectively after 50 years in the natural environment.
- The extrapolated carbonation depth due to unpressurised 100% CO_2 testing could be used for estimating the actual carbonation depth of concrete that has a high resistance to carbonation, such as SCC with a strength grade of 50-60 MPa, in a fairly short time. However, carbonation depth results from actual SCC structures should be maintained to check the validity of the predicted results as current SCC installations progressively age.
- The modification of the internal pore structure in LP and FA-SCC matrices after carbonation was more pronounced in comparison with the FA-SF-SCC matrix and this was likely related to the presence of more macro pores before carbonation and the nature of the carbonation products.
- The combined results of the MIP test and SEM observations after carbonation suggesting that the addition of SF could have a positive effect on modifying the internal pore structure while it had a negative effect on the connectivity of the capillary pores after carbonation especially at the micro scale level. Therefore, the permeation characteristics of a concrete cover might be affected in the case of the interaction of carbonation with water or other aggressive substances.
- The two forms of the Ettringite observed in the SEM examinations in the pore structure of the filler-typed SCC after carbonation could play a significant role in

determining the nature of the internal pores and its connectivity after carbonation, especially at the micro level scale.

Acknowledgements

The principle author would like to express his gratitude for his PhD scholarship sponsored by Higher Committee for Education Development in Iraq (HCED). The authors would like to gratefully acknowledge Mr Mick Winfield (Operations Support Manager NTEC, Faculty of Engineering), Mr Richard Blakemore (senior technician for mixtures area of NTEC, Faculty of Engineering) and Miss Nancy Milne (Technician, Faculty of Engineering) for their help in in manufacturing the normal pressure carbonation chamber, utilizing the pressurized carbonation chamber and cutting the concrete samples. The authors wish also thanks Mr Keith Dinsdale (Chief Experimental Officer, University of Nottingham - Faculty of Engineering), Miss Vikki Archibald (Analytical Technician, University of Nottingham- Faculty of Engineering) and Dr Nigel Neate (University of Nottingham - Faculty of Engineering) for their help in conducting the MIP, TGA and SEM tests.

Captured figures

Fig.1 Schematic diagram and photograph of the normal pressurized accelerated carbonation test with 100% CO_2

Fig.2 Schematic diagram of the pressurized accelerated carbonation test with 100% CO_2 and the samples used

Fig.3 Phenolphthalein carbonation depth measurements

Fig.4 carbonation depth of SCC and mortars versus the exposure time

Fig.5 Carbonation depths versus the square root of time (year) relationships

Fig.6 CO_2 concentration increase in atmosphere from 1955 to June 2013

Fig.7 LP-SCC matrix: (a) MIP intrusion volume against the pore diameter (b) frequency distribution of the pores

Fig.8 Frequency distribution of the pore before and after carbonation (a) FA-SCC matrix (b) FA-SF-SCC matrix

Fig.9 Quantitative analysis of pores percentages change % versus the pores ranges before and after carbonation MIP test

Fig.10 Morphology of capillary pore-structure at 28 days before carbonation (No presence of Ettringite (a) LP-SCC (b) FA-SF-SCC

Fig.11 Monosufate form after carbonation in the pores of (a) LP-SCC (b) FA-SCC

Fig.12 DEF (Ettringite) after carbonation in the pores of FA-SF-SCC (a) low magnification (b) high magnification

Tables

Table 1 Concrete mix designs

Concrete ID	LP-SCC	FA-SCC	FA-SF-SCC
Cement (kg/m^3)	300	300	300
Coarse aggregate (kg/m^3)	860	825	825
Fine aggregate (kg/m^3)	900		
Water (kg/m^3)	180		
Fly ash (kg/m^3)	---	150	120
Limestone (kg/m^3)	150	---	---
Silica fume (kg/m^3)	---	----	30
SP % by weight	2.6	1.83	3.1
Slump flow	700	720	680
T_{50} (sec)	4.5	3.2	3.6
Compressive strength 28 day MPa	57.9	56.5	50

Table 2 CH % content of the mixes at 28 days

Mix ID	LP-SCC	FA-SCC	FA-SF-SCC
CH % dehydration	6.3	4.7	4.2

Table 3 Predicted carbonation depths for SCC in natural environment

Mix ID	$K_{acc.}$ mm/(year)^1/2	$K_{act.}$ mm/(year)^1/2	Carbonation depth (mm) after number of years				
			10	20	30	40	50
LP-SCC	38.6	0.77	2.43	3.44	4.22	4.87	5.44
FA-SCC	32.6	0.65	2.05	2.91	3.56	4.11	4.60
FA-SF-SCC	25.5	0.51	1.61	2.28	2.79	3.22	3.61

Table 4 Micro, macro pores and CPD before and after carbonation of the mixes

Mix ID	Before carbonation			After carbonation		
	Macro pores %	Macro pores %	CPD (μm)	Macro pores %	Macro pores %	CPD (μm)
LP-SCC	66.7	33.3	0.06	78.7	21.3	0.027
FA-SCC	75	25	0.038	77.3	22.7	0.027
FA-SF-SCC	71	29	0.031	79.5	20.5	0.038

Captured figures

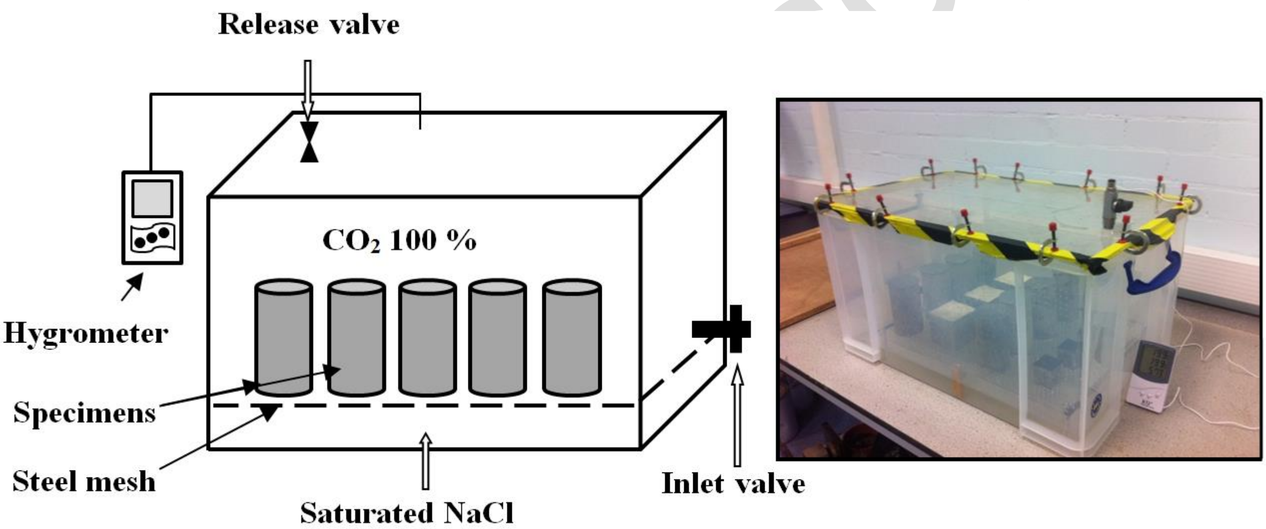

Fig.1 Schematic diagram and photograph of the normal pressurized accelerated carbonation test with 100% CO_2

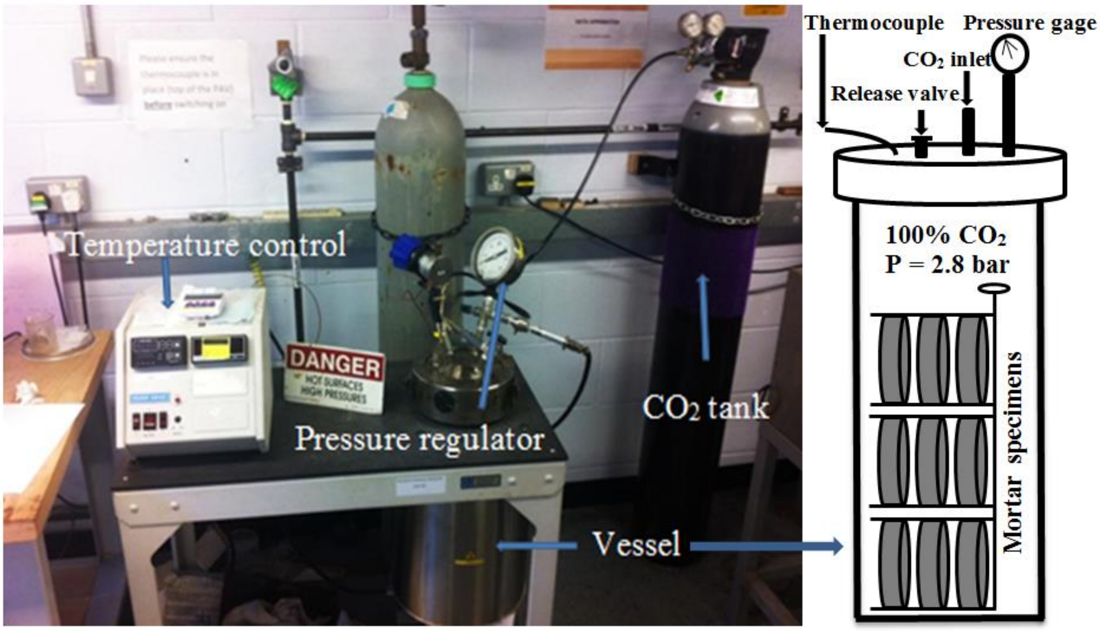

Fig.2 Schematic diagram of the pressurized accelerated carbonation test with 100% CO_2 and the samples used

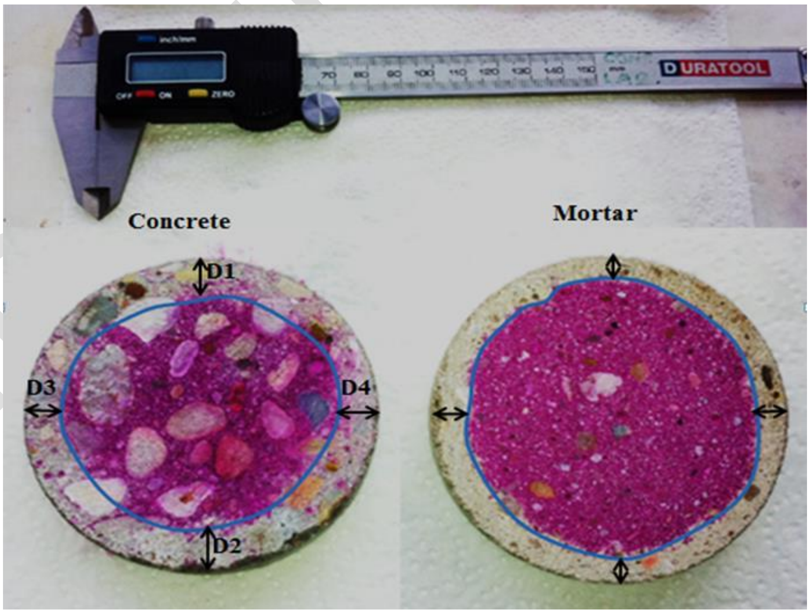

Fig.3 Phenolphthalein carbonation depth measurements

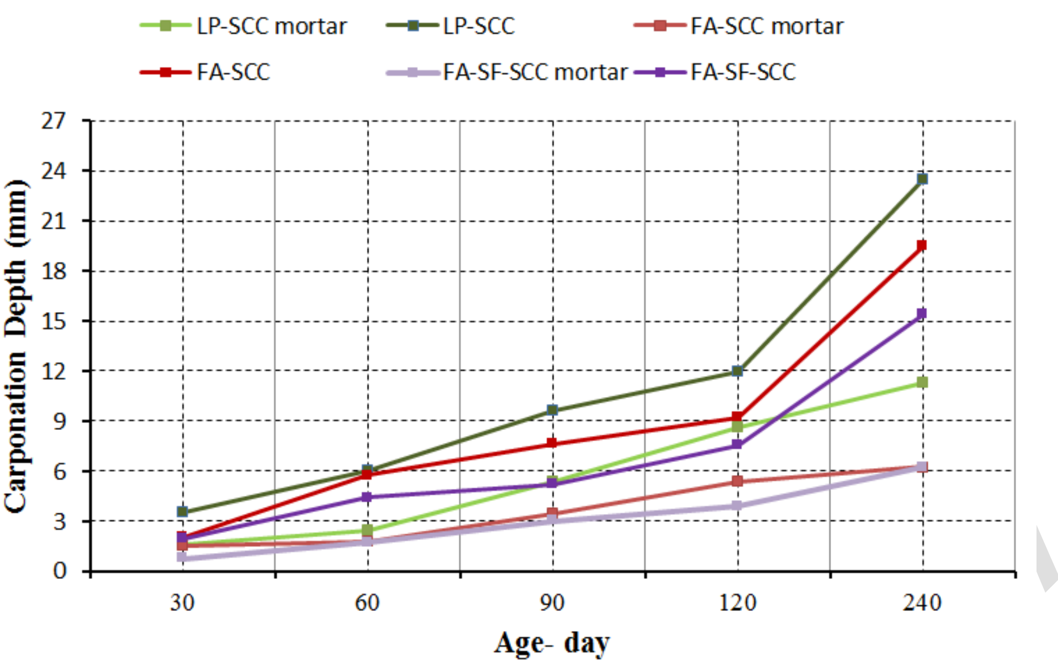

Fig.4 carbonation depth of SCC and mortars versus the exposure time

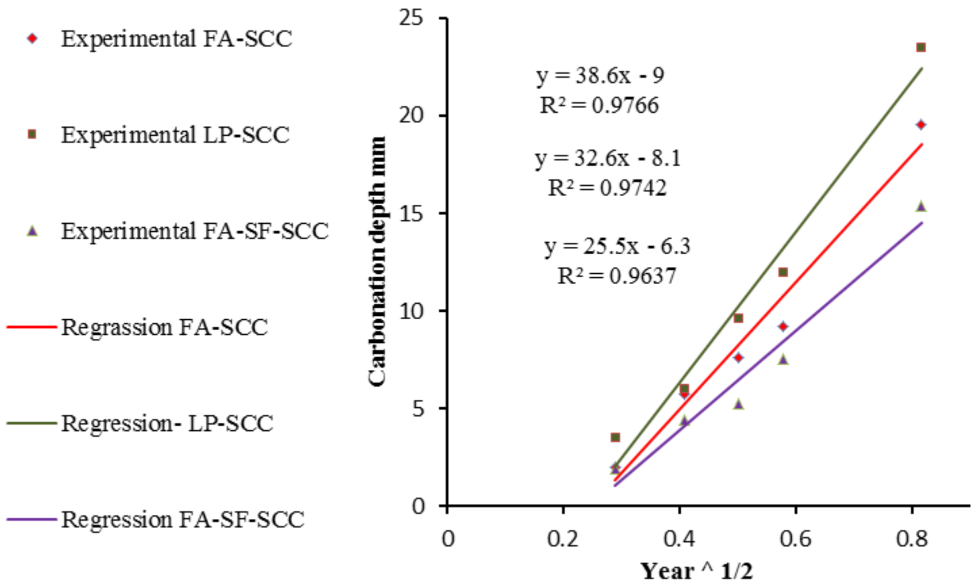

Fig.5 Carbonation depths versus the square root of time (year) relationships

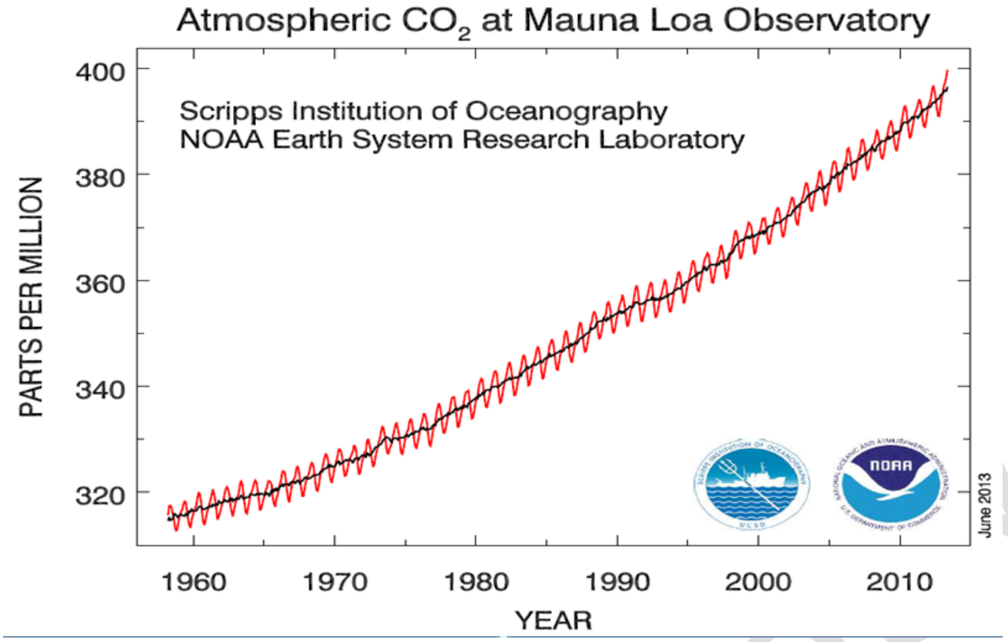

Fig.6 CO_2 concentration increase in atmosphere measured at Mauna Loa observatory from 1955 to June 2013 [28]

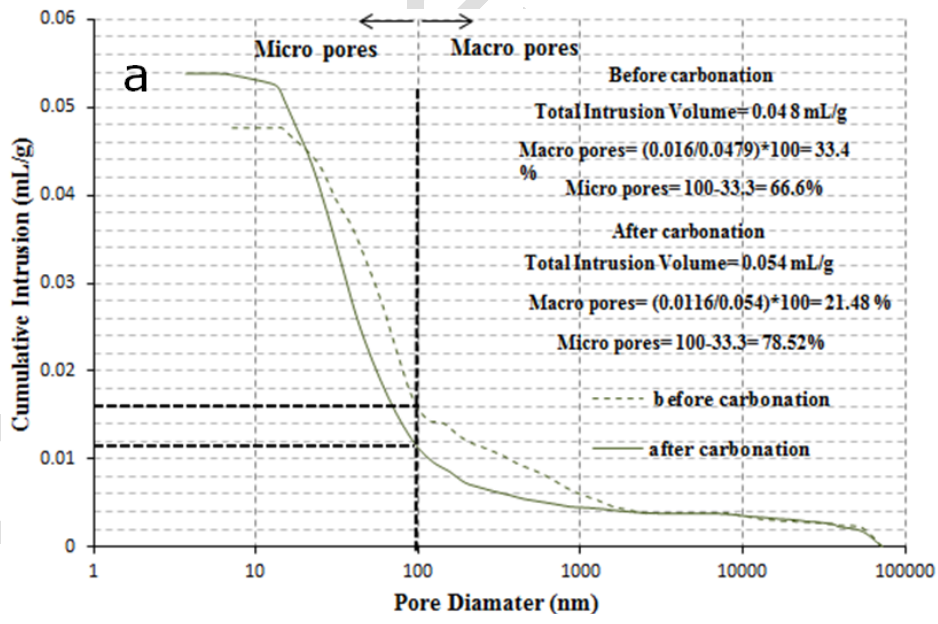

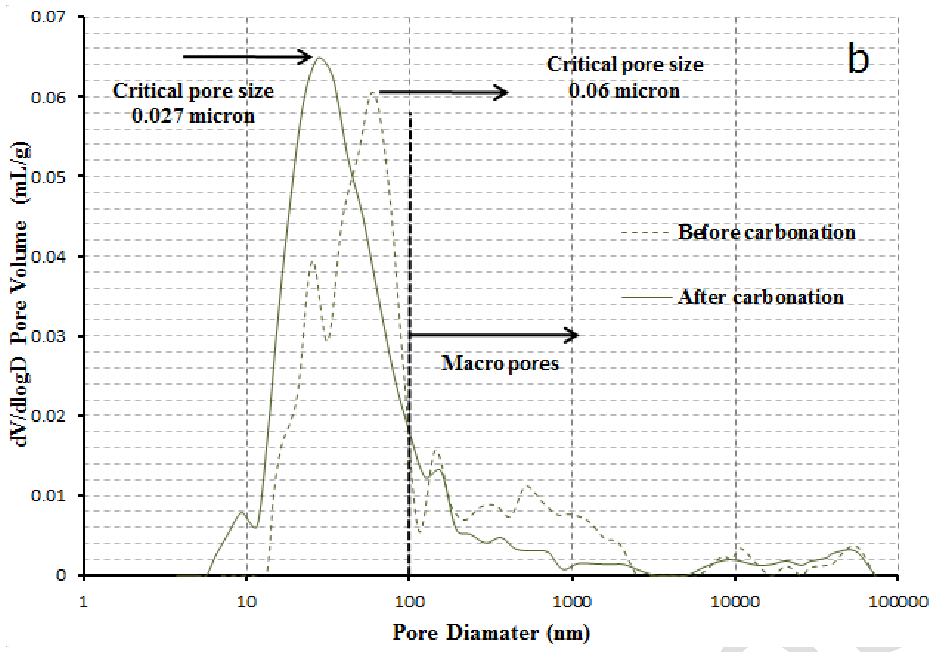

Fig.7 LP-SCC matrix: (a) MIP intrusion volume against the pore diameter (b) frequency distribution of the pores

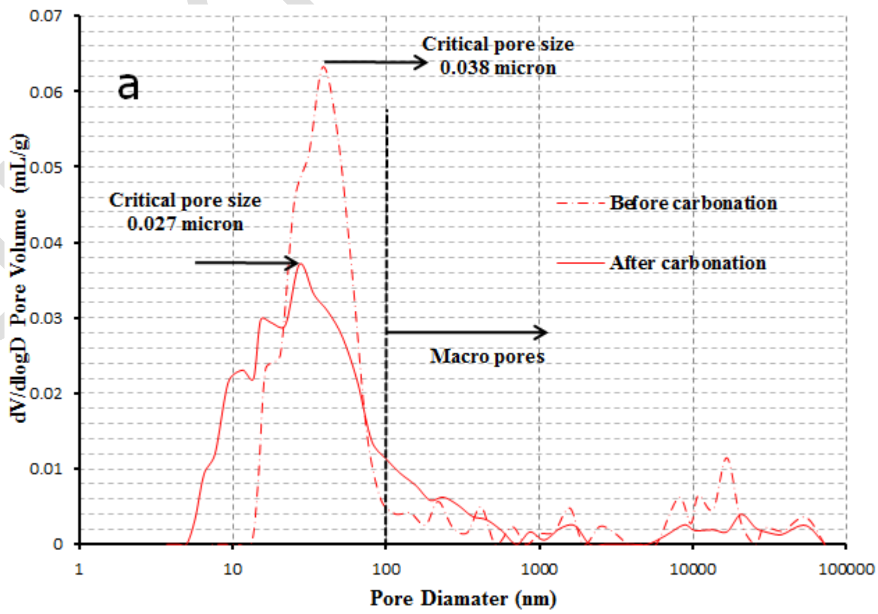

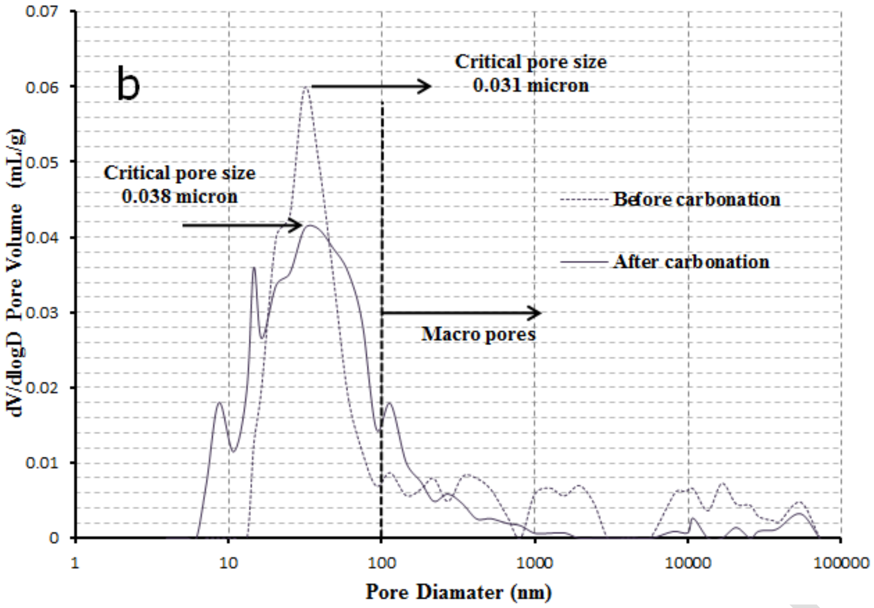

Fig.8 Frequency distribution of the pore before and after carbonation (a) FA-SCC matrix (b) FA-SF-SCC matrix

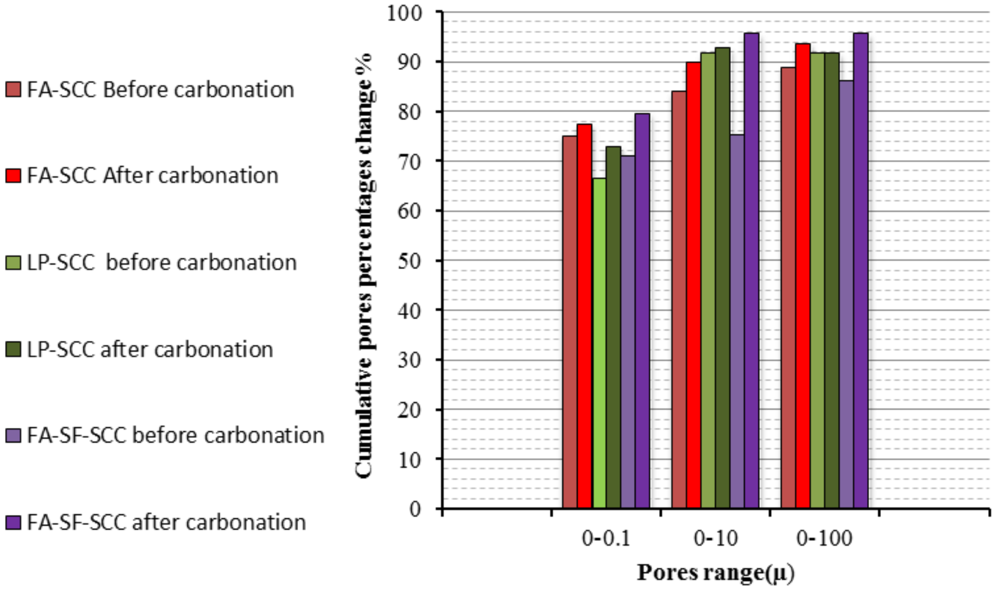

Fig.9 Quantitative analysis of pores percentages change % versus the pores ranges before and after carbonation MIP test

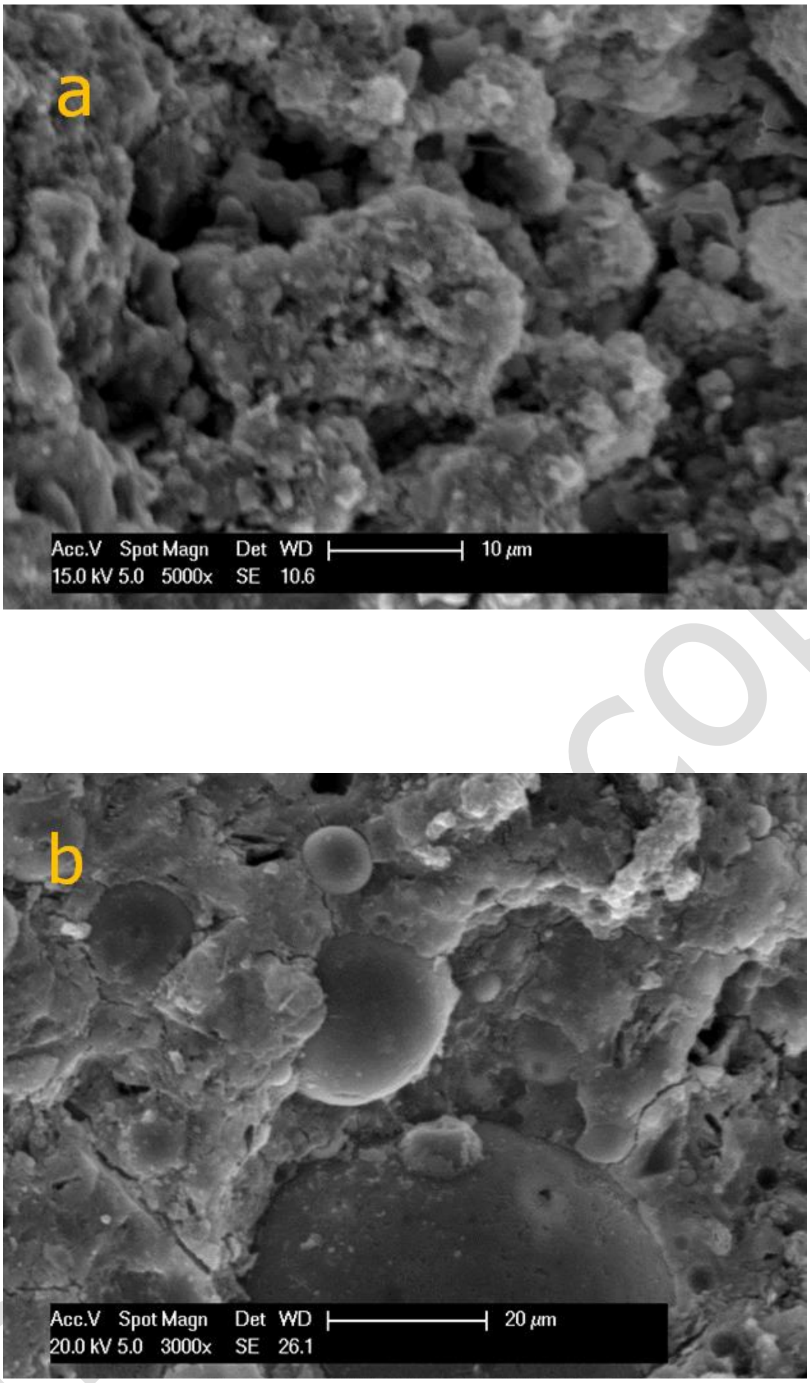

Fig.10 Morphology of capillary pore-structure at 28 days before carbonation (No presence of Ettringite (a) LP-SCC (b) FA-SF-SCC

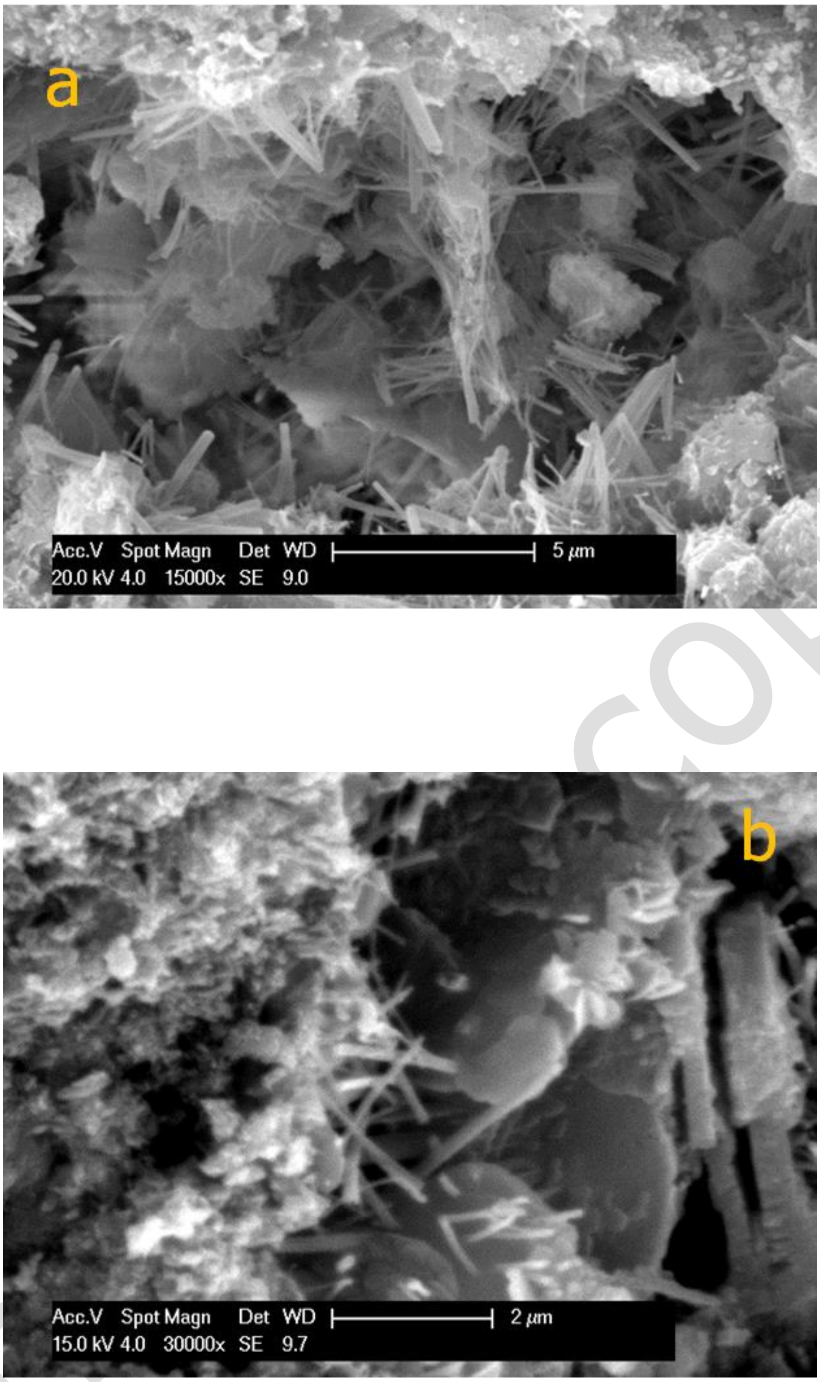

Fig.11 Monosufate form after carbonation in the pores of (a) LP-SCC (b) FA-SCC

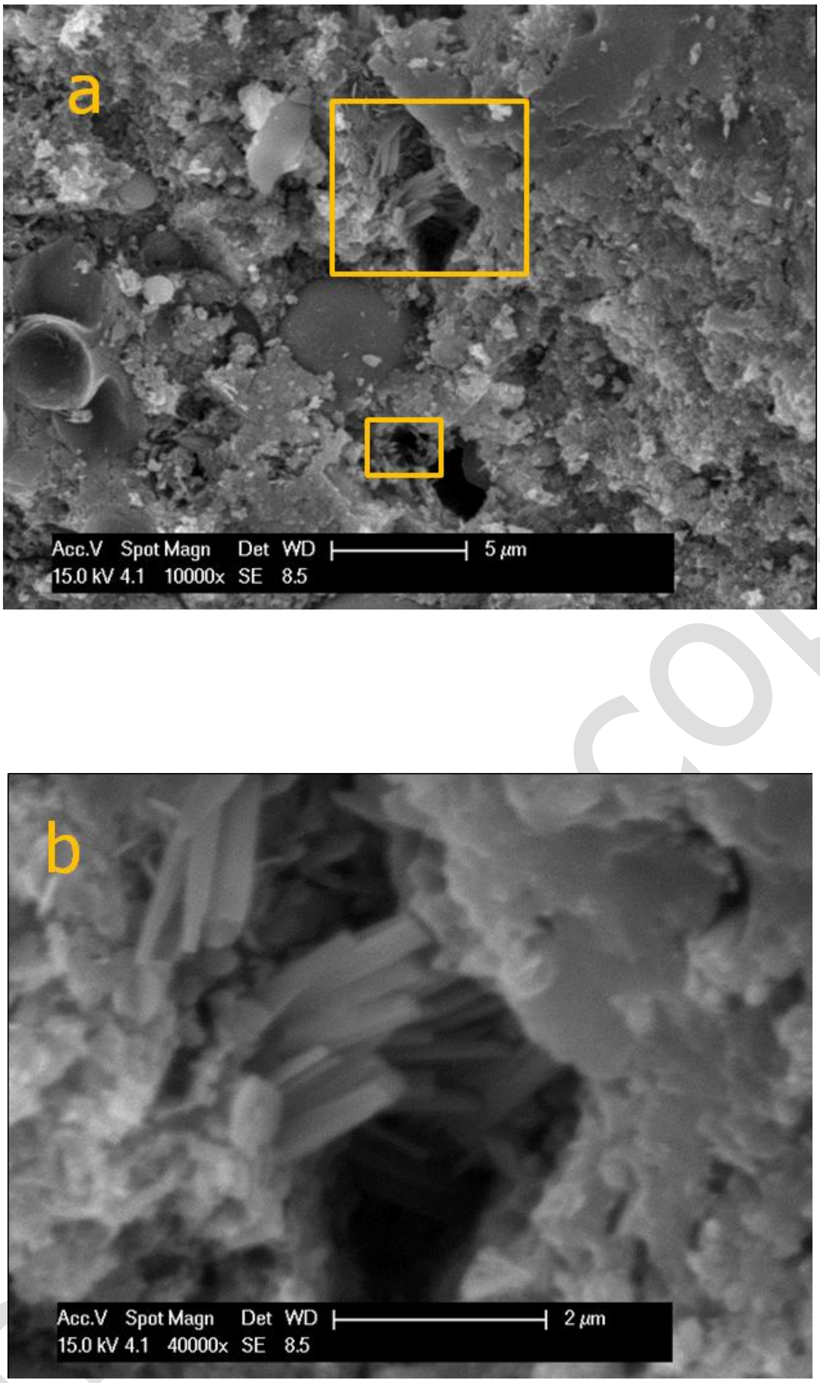

Fig.12 DEF (Ettringite) after carbonation in the pores of FA-SF-SCC (a) low magnification (b) high magnification

References

1. De Schutter, G., K. Audenaert, V. Boel, L. Vandewalle, G. Heirman, J. Vantomme, and J. D'hemricourt. *Transport properties in self-compacting concrete and relation with durability-overview of a Belgian research project (keynote paper)*. in *Proc. of the 3rd Int. Symp. on Self-Compacting Concrete (SCC2003)*. 2003.
2. Nehdi, M., M. Pardhan, and S. Koshowski, *Durability of self-consolidating concrete incorporating high-volume replacement composite cements.* Cement and Concrete Research, 2004. **34**(11): p. 2103-2112.
3. Bassuoni, M. and M. Nehdi, *Durability of self-consolidating concrete to different exposure regimes of sodium sulfate attack.* Materials and Structures, 2009. **42**(8): p. 1039-1057.
4. Chang, J.J., W. Yeih, R. Huang, and C.T. Chen, *Suitability of several current used concrete durability indices on evaluating the corrosion hazard for carbonated concrete.* Materials chemistry and physics, 2004. **84**(1): p. 71-78.
5. Chang, J.J., W. Yeih, R. Huang, and J.M. Chi, *Mechanical properties of carbonated concrete.* Journal of the Chinese Institute of Engineers, 2003. **26**(4): p. 513-522.
6. RILEM, *Final report of RILEM TC 205-DSC: durability of self-compacting concrete, Materials and Structures,2008, P. 225-233.*
7. Parrott, L. *Measurement and modeling of porosity in drying cement paste*. in *Microstructural Development During Hydration of Cement, Mater Res Soc Symp Proc*. 1987: Cambridge Univ Press.
8. Patel, R.G., L.J. Parrott, J.A. Martin, and D.C. Killoh, *Gradients of microstructure and diffusion properties in cement paste caused by drying.* Cement and Concrete Research, 1985. **15**(2): p. 343-356.
9. Wowra, O. *Effects of carbonation to micro structure and pore solution*. in *Proceedings of the RILEM workshop on Frost Resistance of Concrete, Germany*. 2002.
10. Song, H.-W. and S.-J. Kwon, *Permeability characteristics of carbonated concrete considering capillary pore structure.* Cement and Concrete Research, 2007. **37**(6): p. 909-915.
11. Al-Kadhimi, T., P. Banfill, S. Millard, and J. Bungey, *An accelerated carbonation procedure for studies on concrete.* Advances in Cement Research, 1996. **8**(30): p. 47-59.
12. De Schutter, G. and K. Audenaert *Report 38: Durability of Self-Compacting Concrete-State-of-the-Art Report of RILEM Technical Committee 205-DSC*. 2007: RILEM publications.

13. Stehlik, M. and J. Novak, *Verification of the effect of concrete surface protection on the permeability of acid gases using accelerated carbonation depth test in an atmosphere of 98% CO2.* Ceramics–Silikáty, 2011. **55**(1): p. 79-84.

14. Borges, P.H.R., J.O. Costa, N.B. Milestone, C.J. Lynsdale, and R.E. Streatfield, *Carbonation of CH and C–S–H in composite cement pastes containing high amounts of BFS.* Cement and Concrete Research, 2010. **40**(2): p. 284-292.

15. Ngala, V. and C. Page, *Effects of carbonation on pore structure and diffusional properties of hydrated cement pastes.* Cement and Concrete Research, 1997. **27**(7): p. 995-1007.

16. Sanjuan, M., C. Andrade, and M. Cheyrezy, *Concrete carbonation tests in natural and accelerated conditions.* Advances in Cement Research, 2003. **15**(4): p. 171-180.

17. BS EN 13295, *Test method determination of carbonation*. 2004.

18. Roy, S., K. Poh, and D. Northwood, *Durability of concrete—accelerated carbonation and weathering studies.* Building and environment, 1999. **34**(5): p. 597-606.

19. Atiş, C.D., *Accelerated carbonation and testing of concrete made with fly ash.* Construction and Building Materials, 2003. **17**(3): p. 147-152.

20. Khunthongkeaw, J., S. Tangtermsirikul, and T. Leelawat, *A study on carbonation depth prediction for fly ash concrete.* Construction and Building Materials, 2006. **20**(9): p. 744-753.

21. Sisomphon, K. and L. Franke, *Carbonation rates of concretes containing high volume of pozzolanic materials.* Cement and Concrete Research, 2007. **37**(12): p. 1647-1653.

22. Stehlik, M. and J. Novak, *Verification of the effect of concrete surface protection on the permeability of acid gases using accelerated carbonation depth test in an atmosphere of 98%* Ceramics–Silikáty, 2011. **55**(1): p. 79-84.

23. Gonen, T. and S. Yazicioglu, *The influence of compaction pores on sorptivity and carbonation of concrete.* Construction and Building Materials, 2007. **21**(5): p. 1040-1045.

24. Kubo, J., *Methods of remedial treatment for carbonation-induced corrosion of reinforced concrete*. 2007, University of Leeds.

25. RILEM Recommendation CPC-18, *CPC-18 Measurement of hardened concrete carbonation depth.* Mater. Struct, 1988. **21**(6): p. 453-455.

26. Shi, X., N. Xie, K. Fortune, and J. Gong, *Durability of steel reinforced concrete in chloride environments: An overview.* Construction and Building Materials, 2012. **30**: p. 125-138.

27. Bertolini, L., B. Elsener, P. Pedeferri, and R.B. Polder, *Corrosion of steel in concrete: prevention, diagnosis, repair*. 2004: WILEY-VCH.
28. ESRL. *Earth System Research Laboratory;U.S. Department of Commerce*. 2013 [cited 17/06/2013; Available from: http://www.esrl.noaa.gov/gmd/ccgg/trends/.
29. Taylor, H., C. Famy, and K. Scrivener, *Delayed ettringite formation.* Cement and concrete research, 2001. **31**(5): p. 683-693.